DOI 10.5012/bkcs.2010.31.10.2884

Red Fluorescent Organic Light-Emitting Diodes Using Modified Pyran-containing DCJTB Derivatives

Kum Hee Lee, Sung Min Kim, Jeong Yeon Kim, Young Kwan Kim,† and Seung Soo Yoon*

*Department of Chemistry, Sungkyunkwan University, Suwon 440-746, Korea. *E-mail: ssyoon@skku.edu*
†Department of Information Display, Hongik University, Seoul 121-791, Korea
Received July 16, 2010, Accepted September 2, 2010

Two red fluorescent DCJTB derivatives (**Red 1** and **2**) based on modified pyrans were synthesized and their electroluminescent properties were investigated. Multilayered OLEDs were fabricated with the device structure of ITO/NPB (40 nm)/**Red 1**, **2** or **DCJTB** (0.5 or 1%): Alq_3 (20 nm)/Alq_3 (40 nm)/Liq (2 nm)/Al. All devices exhibited efficient red emissions. In particular, a device containing emitter **Red 2** as a dopant in the emitting layer, the maximum luminance was 8737 cd/m^2 at 12.0 V, the luminous and power efficiencies were 2.31 cd/A and 1.25 lm/W at 20 mA/cm^2, respectively. The peak wavelength of the electroluminescence was 638 nm with the CIE (x,y) coordinates of (0.63, 0.36) at 7.0 V.

Key Words: OLED, Red fluorescence, DCJTB derivatives, Pyran

Introduction

Recently, organic light-emitting diodes (OLEDs) have attracted much scientific and commercial interest because of their potential application in full-color displays.[1-3] Due to the requirements for full-color displays, considerable research have been focused on the developments in sets of the primary color emitters of red, green, and blue (RGB). A variety of fluorescent emitters for OLEDs have been developed since reports from Kodak.[4] While blue and green fluorescent emitters showed the sufficient EL performances for applications in flat-panel displays,[5] red fluorescent emitters are still necessary to improve their electroluminescent properties.[6-10] In general, the DCM derivatives have electron donor-acceptor structures with narrow band gap. In most DCM type emitters, concentration quenching due to excimer and exciplex formation dramatically reduces EL performance.[11] Therefore, there have been considerable efforts to develop the efficient red fluorescent materials by preventing excimer and exciplexes formation through incorporation of sterically bulky moieties in DCM type emitters. In particular, DCJTB (4-(dicyanomethylene)-2-*tert*-butyl-6-(1,1,7,7-tetramethyljulolidyl-9-enyl)-4*H*-pyran)[12] have been widely used as red emitters for OLEDs applications due to their high photoluminescent (PL) quantum yields. In these materials, *tert*-butyl groups on pyran moiety have large steric hindrance due to its non-coplanar configuration, leading to reduce the molecular aggregation in the solid state. However, red fluorescent emitters require further improvement in terms of efficiency, lifetime, and color chromaticity.

In this paper, a series of red fluorescent emitters 2-Adamantyl-6-(3,3,7,7-tetrametyljulolidyl)vinyl-4-(2-methylenemalononitrilyl)-4*H*-pyran (**Red 1**) and 2-Adamantyl-6-(3,3,7,7-tetrametyljulolidyl)vinyl-4-(2-methylene-1,3-indanedione)-4*H*-pyran (**Red 2**) based on modified pyrans were synthesized and their electroluminescent properties were investigated. Red emitters **Red 1** and **2** have DCJTB type donor-acceptor emitting cores. In pyran moieties of **Red 1** and **2**, the bulky adamantane groups are incorporated to prevent molecular aggregation between emitters and thus reduce concentration quenching.[13,14] Additionally, to control the color purities, 1,3-indanedione are introduced in pyran moieties of **2**.

Experimental Details

Materials and measurements. Schemes of synthesized red dopant materials (**Red 1** and **2**) are shown in Scheme 1. The red compounds have proper yield and purification. ^{1}H-NMR and ^{13}C-NMR were recorded on a Varian (300 or Unity Inova 300Nb or Unity Inova 500Nb) spectrometer. The FT-IR spectra recorded using a Buuker VERTEX70 FT-IR spectrometer. Low-resolution mass and high-resolution mass spectra were measured using a Jeol JMS-AX505WA spectrometer in the FAB mode and a Jeol JMS-600W spectrometer in the EI mode and JMS-T100TD (AccuTOF-TLC) in the positive ion mode. The UV-vis absorption and photoluminescence spectra of these newly designed red dopants were measured in 10^{-5} M dilute 1,2-dichloroethane. The fluorescent quantum yields were determined in 1,2-dichloroethane at 293 K against DCJTB (Φ = 0.78). The HOMO energy levels were measured with a low energy photo-electron spectrometry (Riken-Keiki AC-2). LUMO energy levels were estimated by subtracting the energy gap from the HOMO energy levels.

2-Adamantyl-6-(3,3,7,7-tetrametyljulolidyl)vinyl-4-(2-methylenemalononitrilyl)-4*H*-pyran (Red 1): 3,3,7,7-tetramethyljulolidinylaldehyde (0.97 mmol) and **1** (1.07 mmol), and piperidine (9.71 mmol) were dissolved in ethanol (12 mL) and refluxed for overnight under nitrogen. After solution cooled, the solid was filtered and re-dissolved into ethyl acetate, washed with water, and separated. The combined extracts were dried (Mg_2SO_4) and concentrated under reduced pressure. The crude product was purified by recrystallized from methylene chloride/hexane to give **Red 1** of red solid. (Yield: 71%) ^{1}H-NMR (300 MHz, $CDCl_3$) δ 7,31 (s, 1H), 7.26 (s, 1H), 6.59 (s, 1H), 6.44 (t, J = 7.8 Hz, 3H), 3.30 (t, J = 5.9 Hz, 4H), 2.16 (s, 3H), 1.98 (s,

6H), 1.86-1.74 (m, 10H), 1.32 (s, 12H), ^{13}C-NMR (125 MHz, $CDCl_3$) δ 171.9, 161.0, 157.1, 143.1, 139.5, 130.5, 124.4, 121.3, 116.5, 116.4, 111.7, 105.2, 102.7, 101.5, 56.8, 46.9, 40.1, 38.5, 36.5, 32.4, 30.6, 28.1, FT-IR (KBr) ν 2360, 1653, 1617, 1542, 1496, 1472, 1465, 1179, 668, MS (EI^+) (*m*/*z*) 531 [M^+]; HRMS (TOF^+): [M^++H] calcd for $C_{36}H_{42}NO_3$, 532.3328; Found, 532.3300, mp 302 - 303 °C.

2-Adamantyl-6-(3,3,7,7-tetrametyljulolidyl)vinyl-4-(2-methylene-1,3-indanedione)-4*H*-pyran (Red 2): Compound **Red 2** was prepared by method of **Red 1** using **1** instead of **2**. The obtained product was red solid. (Yield: 78%) ^{1}H-NMR (300 MHz, $CDCl_3$) δ 8.39 (d, *J* = 19.6 Hz, 2H), 7.75-7.71 (m, 2H), 7.60-7.56 (m, 3H), 7.33 (d, *J* = 15.8 Hz, 2H), 6.64 (d, *J* = 15.8 Hz, 1H), 3.29 (t, *J* = 5.7 Hz, 4H), 2.17 (s, 3H), 2.07 (s, 6H), 1.83-1.75 (m, 10H), 1.34 (s, 12H), ^{13}C-NMR (125 MHz, $CDCl_3$) δ 193.2, 173.7, 163.4, 150.2, 142.8, 140.9, 138.3, 133.0, 130.5, 124.3, 121.8, 121.2, 113.7, 107.5, 103.9, 46.9, 40.3, 38.8, 36.7, 36.2, 32.4, 30.8, 28.3, FT-IR (KBr) ν 1684, 1496, 1317, 668, MS (FAB^+) (*m*/*z*) 612 [M^+]; HRMS (TOF^+): [M^++H] calcd for $C_{42}H_{46}NO_3$, 612.3478; Found, 612.3474, mp 197 - 198 °C.

Device fabrication and characterization. All processes were carefully produced. Before the indium tin oxide (ITO) was doped, acetone, methyl alcohol, distilled water, and kept in isopropyl alcohol for 48 h and dried by N_2 gas. The ITO deoxidized condition in vaccum and then in order of *N*,*N*′-diphenyl-*N*,*N*′-(1-naphthyl)-(1,1'-phenyl)-4,4'-diamine (NPB), Red dopant and tris(8-quionlinolato)-aluminium (Alq_3), Alq_3, Al doped. The optimization of EL devices have structure of ITO/NPB (40 nm)/Red dopants (0.5 or 1%): Alq_3 (20 nm)/Alq_3 (40 nm)/Liq (2 nm)/Al. The current density (J), luminance (L), luminous efficiency (LE), power efficiency (PE) and the CIE chromaticity coordinates of the OLEDs were measured with Keithly 2400, Chroma meter CS-1000A. Electro-luminance was measured using a Roper Scientific Pro 300i.

Results and Discussion

The structures of Red dopants (**Red 1** and **Red 2**) were shown in Figure 1. Also, synthesized Red dopants (**Red 1** and **Red 2**) were shown in Scheme 1. After the conventional purifications such as column chromatography and recrystallization, these newly synthesized red-emitting materials (**Red 1** and **Red 2**) were purified further by train sublimation at the reduced pressure below 10^{-3} torr and fully characterized with ^{1}H- and ^{13}C-NMR, infrared (IR), and low- and high-resolution mass spectrometry. High-pressure liquid chromatography (HPLC) analysis was carried out to check the purity of materials. These analyses revealed that the purity of red-emitting materials (**Red 1** and **Red 2**) is at least above 99.0%. The ultraviolet-visible

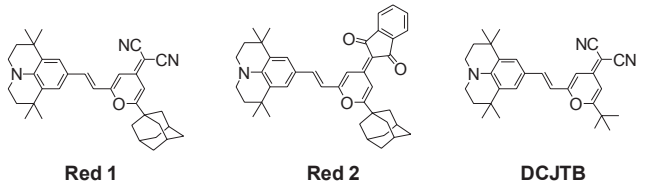

Figure 1. The structures of **Red 1**, **Red 2** and **DCJTB**.

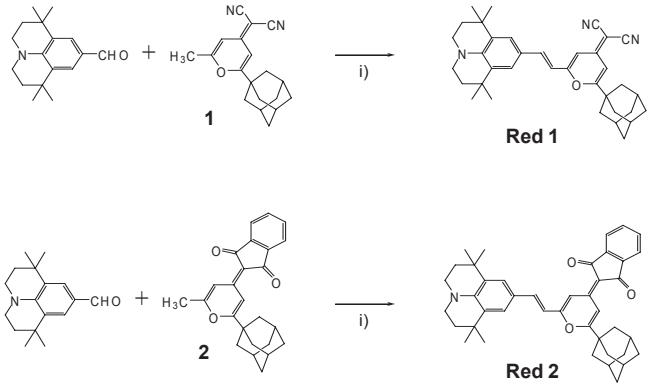

Scheme 1. Synthesis of **Red 1** and **Red 2**. **i**) Piperidine, EtOH

(UV-vis) absorption and photoluminescence (PL) spectra of red dopant materials **Red 1** and **Red 2** as shown in Figure 2. The maximum absorption peaks of **Red 1** and **Red 2** were 512 nm and 545 nm, respectively. There are the good spectral overlap between the emission of the common host (Alq_3) and the absorption of **Red 1** and **Red 2**. This indicates that Alq_3 served well as a host in the OLEDs by using these compounds **Red 1** and **Red 2** as red dopant materials. The maximum emission peaks of **Red 1** and **Red 2** appeared at 617 and 656 nm, respectively, in the visible spectrum of red region. Compare to **Red 1**, the ab-

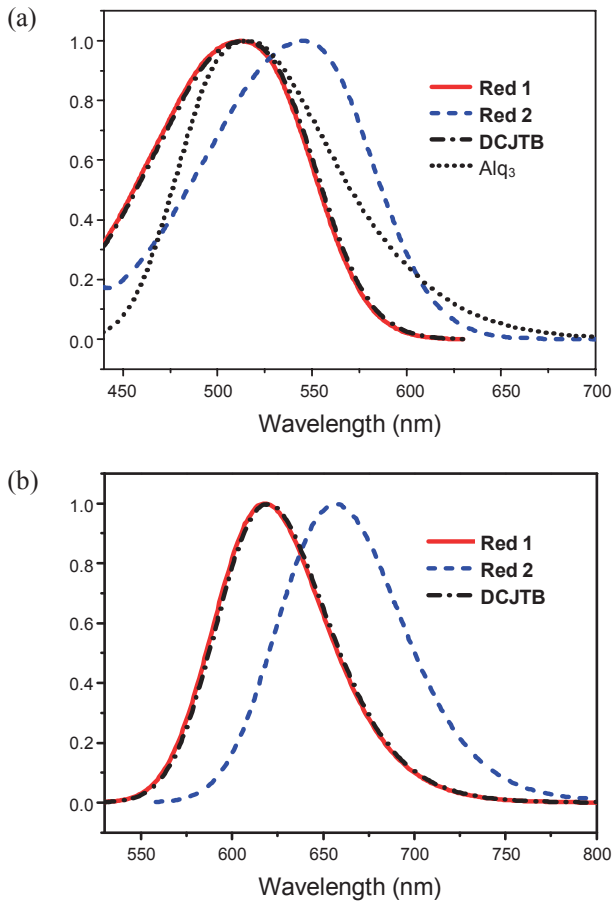

Figure 2. (a) UV-vis absorption spectra and (b) Photoluminescence spectra of **Red 1** and **Red 2**.

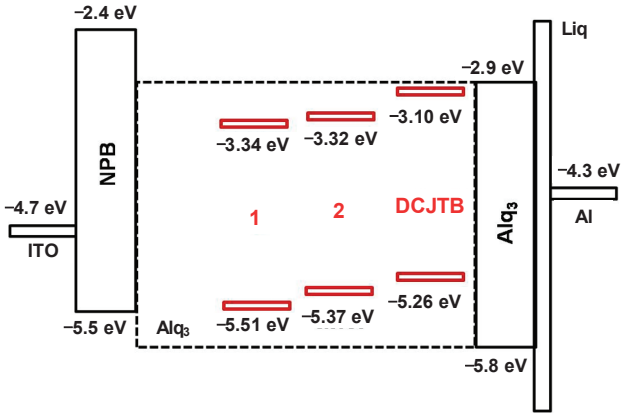

Figure 3. Energy-level diagram of red OLEDs.

sorption and PL spectra of **Red 2** show bathochromic shift due to the lengthening π-conjugation length by 1,3-indanedione moiety. The PL quantum yields of **Red 1** and **Red 2** were measured in 1,2-dichloroethane, using **DCJTB** as a standard, and those were 0.76 and 0.85, proper quantum yields as dopant materials, respectively. The highest occupied molecular orbital (HOMO) level was measured with a photoelectron spectrometer used to Riken-Keiki AC-2 and lowest occupied molecular orbital (LUMO) level was computed by optical band gap energy and HOMO level. The HOMO and LUMO energy levels for **Red 1** and **Red 2** are −5.37 to −5.51 eV and −3.32 to −3.35 eV, respectively.

The device structure and HOMO/LUMO energy levels of the materials in device are shown in Figure 3. NPB was introduced as hole-transporting layer (HTL) to enhanced hole injection and transport, Alq_3 functioned as emitting layer (EML) as well as electron-transporting layer (ETL).

Red devices with a structure ITO/NPB (40 nm)/Alq_3: red dopant (0.5 or 1%) (20 nm)/Alq_3 (40 nm)/Liq (2 nm)/Al were fabricated to explore the electroluminescence (EL) properties of the dopant materials. The (a) current density-voltage (*I-V*) and (b) luminance-voltage characteristics (*L-V*) of the devices **1-4** are shown in Figure 4. The maximum luminances of the devices are 1658, 8737, 4000, and 6300 cd/m^2, respectively.

The luminous efficiency and power efficiency-current density characteristics of devices **1-4** are shown in Figure 5 and 6, respectively. The luminance efficiencies of devices **1-4** were 2.44, 2.31, 1.02, and 2.45 cd/A at 20 mA/cm^2, respectively. The power efficiencies of devices **1-4** were 0.87, 1.25, 0.53, and

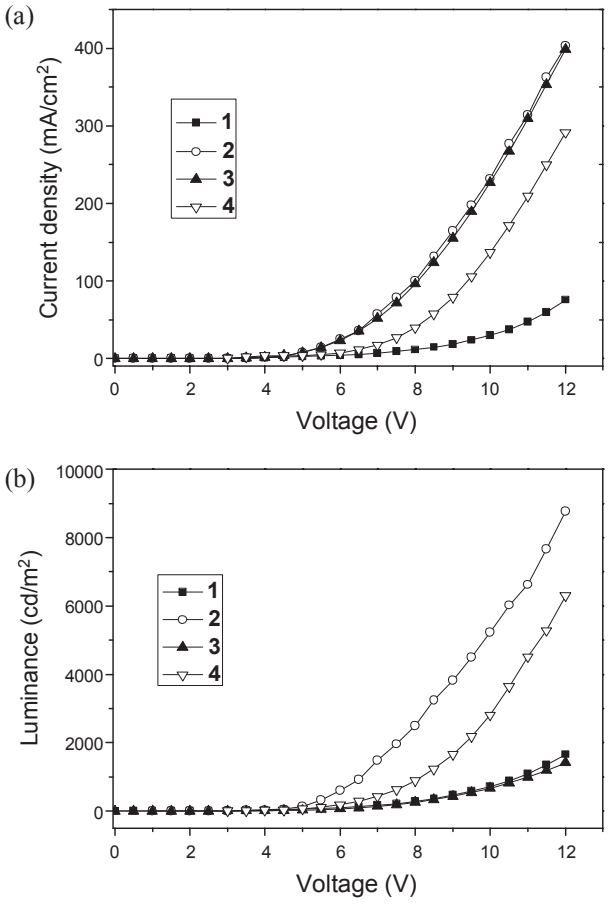

Figure 4. (a) Current density-Voltage (b) Luminance-Voltage characteristics of devices **1-4**.

1.06 lm/W at 20 mA/cm^2, respectively.

At the same 1% doping condition, the EL performances of device **1** using **Red 1** as a dopant is in the similar ranges of those of device **4** using **DCJTB**. These observations imply that the adamantane group and *tert*-butyl group in pyran moiety of dopant in devices **1** and **4**, respectively, have the similar steric effect on the EL perfornamces of OLED devices using them by preventing molecular aggregation between emitters and thus reducing concentration quenching. However, the other factors such as the quantum yields of **Red 1** and **DCJTB** and the degree of overlap of the absorption spectra of **Red 1** and **DCJTB** with the PL spectrum of Alq_3 host could play important roles in the EL performances of device **1** and **4**, because these two photo-

Table 1. Physical properties of **Red 1** and **Red 2**

Com	UV_{Max} (nm)[a]	PL_{Max} (nm)[a]	FWHM	HOMO (eV)[b]	LUMO (eV)[b]	E_g	Q.Y[c]
Red 1	512	617	72	−5.51	−3.35	2.17	0.76
Red 2	545	656	80	−5.37	−3.32	2.05	0.85
DCJTB	511	620	72	−5.26	−3.10	2.16	0.78

[a,b]Maximum absorption or emission wavelength in 1,2-dichloroethane (*ca.* 1 × 10^{-5} M). [b]Obtained from AC-2 and UV-vis absorption measurements. [c]Using DCJTB as a standard; λ_{ex} = 550 nm (Φ = 0.78 in 1,2-dichloroethene).

Table 2. EL performance characteristic of devices **1-4**

Device	Dopant (doping %)	L[a] (cd/m^2)	LE-J[b] (cd/A)	PE[b] (lm/w)	EL[c] (nm)	CIE[c] (x,y)
1	**Red 1** (1%)	1658	2.44	0.87	616	(0.61, 0.39)
2	**Red 2** (0.5%)	8767	2.31	1.25	638	(0.63, 0.36)
3	**Red 2** (1%)	4000	1.02	0.53	638/682	(0.64, 0.35)
4	**DCJTB** (1%)	6300	2.45	1.06	616	(0.60, 0.39)

[a]Value of the Maximum luminance at 12.0 V, [b]Values measured at 20 mA/cm^2, [c]Value measured at 7.0 V.

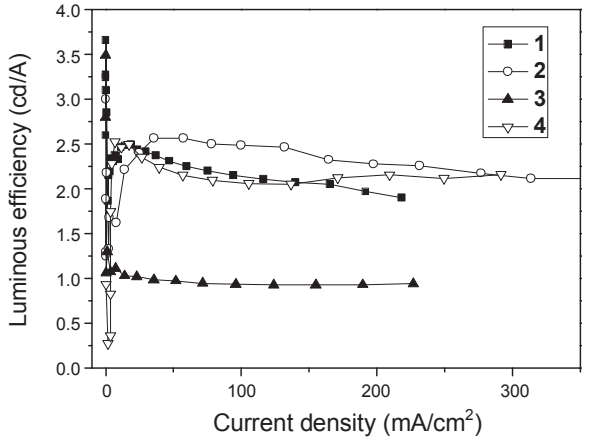

Figure 5. Luminous efficiency-current density characteristics of devices **1-4**.

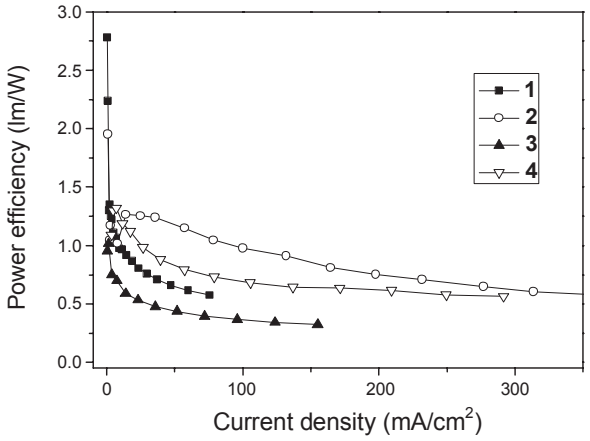

Figure 6. Power efficiency-current density characteristics of devices **1-4**.

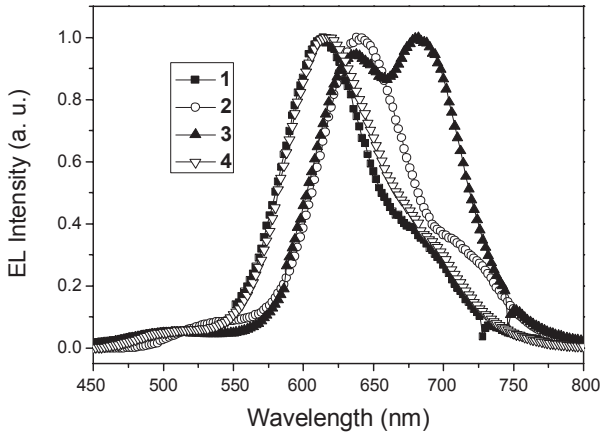

Figure 7. EL spectra of devices **1-4**.

physical properties of **Red 1** and **DCJTB** are similar to each other. Interestingly, although the HOMO/LUMO energy levels of **Red 1** and **DCJTB** showed the large differences, the EL performances of devices **1** and **4** using them dopants are similar to each other. Presumably, these observations imply that the charge trapping processes by dopants in the emitting layers are ineffective in devices **1** and **4**. Device **3** using **Red 2** as a dopant showed much worse EL efficiencies than device **1** at the same 1% doping concentration due to the effective molecular aggregation and thus excimer formation of **Red 2**. Notably, compared to device **3** using **Red 2** as a dopant at 1% concentration, the luminous efficiency and power of device **2** using the same dopant at 0.5% concentration increased by 127% and 136% at 20 mA/cm^2, respectively. At the lower doping concentration, molecular aggregation between dopants and thus the excimer formation in the emitting layer reduced and lead to the improved EL efficiencies.

The electroluminescent emission spectra of devices **1**-**4** are shown in Figure 7. The EL maximum wavelengths of devices were 616, 638, 638/682 and 616 nm at 7.0 V, respectively. Interestingly, compared to device **2** using dopant **Red 2** at 0.5% concentration, the EL spectrum of device **3** using the same dopant at 1% concentration had a large shoulder at 682 nm due to the excimer formation between dopant **Red 2** in the emitting layer of device **3**. The CIE coordinate of devices are (0.61, 0.39), (0.63, 0.36), (0.64, 0.35) and (0.61, 0.39) at 7.0 V, respectively. Among the devices **1**, **3** and **4** using dopants at the same dopping concentration, device **3** showed the improved color chromaticity due to the lengthening π-conjugation length by 1,3-indanedione moiety of dopant **Red 2**.

Conclusions

Efficient red fluorescent DCJTB derivatives with modified pyran moiety had developed. An OLED device using dopant **Red 2** with the bulky adamantane group and 1,3-indanedione in pyran moiety showed a maximum luminance of 8737 cd/m^2 at 12.0 V, the luminous and power efficiencies were 2.31 cd/A and 1.25 lm/W at 20 mA/cm^2, respectively. The CIE coordinate of this device was (0.63, 0.36) at 7.0 V. The reduced molecular aggregation by the bulky adamantane group and the extended π-conjugation length by 1,3-indanedione group of **Red 2** would lead to the improved EL performances of OLED device using **Red 2** as a dopant. This study suggests that the DCJTB derivatives with modified pyran moiety have the excellent properties for red emitting materials for OLEDs.[15-18]

Acknowledgments. This research was supported by Basic Science Research Program through the NRF funded by the Ministry of Education, Science and Technology (20100007370).

References

1. Tang, C. W.; Van Slyke, S. A. *Appl. Phys. Lett.* **1987**, *51*, 913.
2. Wu, Z.; Jiao, B.; Zhao, X.; Hou, L.; Wang, H.; Gao, Y.; Qiu, Y. *Thin Solid Films.* **2009**, *517*, 3382.
3. Tang, C. W.; VanSlyke, S. A.; Chen, C. H. *J. Appl. Phys*. **1989**, *65*, 3610.
4. Kim, D. U.; Paik, S. H.; Kim, S. -H.; Tsutsui, T. *Synth. Meter.* **2001**, *123*, 43.
5. Lee, K. H.; Kang, L. K.; Lee, J. Y.; Kang, S.; Jeon, S. O.; Yook, K. S.; Lee, J. Y.; Yoon, S. S. *Adv. Funct. Mater.* **2010**, *20*, 1345.
6. Kim, I. H.; Byun, K. N.; Yoo, H. S. *Curr. Appl. Phys.* **2005**, *5*, 345.
7. Zhang, X. H.; Chen, B. J.; Lin, X. Q.; Wong, O. Y.; Lee, C. S.; Kwong, H. L.; Lee, S. T.; Wu, S. K. *Chem. Mater.* **2001**, *13*, 1565.

8. Yao, Y. S.; Zhou, Q. X.; Wang, X. S.; Wang, Y.; Zhang, B. W. *Adv. Funct. Mater*. **2007**, *17*, 93.
9. Zhao, P.; Tang, H.; Zhang, Q.; Pi, Y.; Xu, M.; Sun, R.; Zhu, W. *Dyes. Pigments*. **2009**, *82*, 316.
10. Lee, K. H.; Park, M. H.; Kim, S. M.; Kim, Y. K.; Yoon, S. S. *Jpn. J. Appl. Phys.* **2010**, *49*, 08JG02.
11. Chen, C. H. *Chem. Mater*. **2004**, *16*, 4389.
12. Chen, C. H; Tang, C. W.; Chi, J.; Klubek, K. P. *Thin Solid Films* **2000**, *363*, 327.
13. Li, X.; Wei, D.-Y.; Huang, S.-J.; Zheng, Y.-Q. *J. Solid. State. Chem*. **2009**, *182*, 95.
14. Nematollahi, D.; Akaberi, N. *Molecules* **2001**, *6*, 639.
15. Hata, N.; Tanaka, I. *J. Chem. Phys.* **1962**, *36*, 2072.
16. Förster, T. *Discuss. Faraday Soc*. **1959**, *27*, 7.
17. Dexter, L. D. *J. Chem. Phys*. **1953**, *21*, 836.
18. Rolon, J. E.; Ulloa, S. E. *Phys. Rev. B* **2009**, *79*, 245309.